Embryonic Photosynthesis Affects Post-Germination Plant Growth[1][OPEN]

Ayala Sela,[a] Urszula Piskurewicz,[a] Christian Megies,[a] Laurent Mène-Saffrané,[b] Giovanni Finazzi,[c] and Luis Lopez-Molina[a,d,2,3]

[a]Department of Botany and Plant Biology, University of Geneva, 1211 Geneva, Switzerland
[b]Department of Biology, University of Fribourg, 1700 Fribourg, Switzerland
[c]Université Grenoble Alpes, Centre National de la Recherche Scientifique, Commissariat à l'Énergie Atomique et aux Énergies Alternatives, Institut National de la Recherche Agronomique, Interdisciplinary Research Institute of Grenoble - Cell & Plant Physiology Laboratory, 38000 Grenoble, France
[d]Institute of Genetics and Genomics in Geneva, University of Geneva, 1211 Geneva, Switzerland

ORCID IDs: 0000-0002-9523-9123 (U.P.); 0000-0003-0463-1187 (L.L.-M.).

Photosynthesis is the fundamental process fueling plant vegetative growth and development. The progeny of plants relies on maternal photosynthesis, via food reserves in the seed, to supply the necessary energy for seed germination and early seedling establishment. Intriguingly, before seed maturation, Arabidopsis (*Arabidopsis thaliana*) embryos are also photosynthetically active, the biological significance of which remains poorly understood. Investigating this system is genetically challenging because mutations perturbing photosynthesis are expected to affect both embryonic and vegetative tissues. Here, we isolated a temperature-sensitive mutation affecting *CPN60α2*, which encodes a subunit of the chloroplast chaperonin complex CPN60. When exposed to cold temperatures, *cpn60α2* mutants accumulate less chlorophyll in newly produced tissues, thus allowing the specific disturbance of embryonic photosynthesis. Analyses of *cpn60α2* mutants were combined with independent genetic and pharmacological approaches to show that embryonic photosynthetic activity is necessary for normal skoto- and photomorphogenesis in juvenile seedlings as well as long-term adult plant development. Our results reveal the importance of embryonic photosynthetic activity for normal adult plant growth, development, and health.

Seed development in Arabidopsis (*Arabidopsis thaliana*) is initiated after a double fertilization event, characteristic of flowering plants, which produces the endosperm and the zygote. Seed development can be divided in two phases. The first phase is that of embryogenesis per se, i.e. the zygote undergoes morphogenesis through several rounds of cell division and differentiation. This consists of successive developmental stages, referred to as globular, heart, torpedo, and walking-stick, during which the basic architecture of the plant embryo is established following a pattern organized along an apical-basal and radial axis (ten Hove et al., 2015). Eventually, 8–10 d after fertilization, this first phase ends with the cessation of cell division and the formation of the plant embryo, at which stage the embryo is surrounded by a single cell layer of endosperm. Thereupon, the second phase, or seed maturation phase, is initiated, whereby embryonic cells expand as a result of protein and lipid food reserve accumulation. Acquisition of osmotolerance and seed desiccation is also an important characteristic of seed maturation (Leprince et al., 2017). Eventually, the maturation phase produces a highly resistant and food-rich embryo, which remains surrounded by a single cell layer of mature endosperm. In the mature seed, the living endosperm and embryo tissues are shielded by a protective external layer of dead maternal coat, namely the testa, consisting of differentiated and tannin-rich integumental ovular tissues. Hence, seed development produces a desiccated, metabolically inert, and highly resistant plant embryo that possesses energetic autonomy needed to fuel its germination and early seedling establishment.

Photosynthesis is the fundamental process occurring in plant chloroplasts allowing plants to convert solar energy into chemical energy, which fuels their growth and development (Johnson, 2016). During embryogenesis, the

[1]This work was supported by the Swiss National Science Foundation (grant nos. 31003A-152660/1 and 31003A-179472/1), the State of Geneva, the French National Research Agency, Grenoble Alliance for Integrated Structural Cell Biology (grant no. ANR-10-13 LABEX-04 GRAL Labex to G.F.), and the Interdisciplinary Research Institute of Grenoble.

[2]Author for contact: luis.lopezmolina@unige.ch.
[3]Senior author.

The author responsible for distribution of materials integral to the findings presented in this article in accordance with the policy described in the Instructions for Authors (www.plantphysiol.org) is: Luis Lopez-Molina (luis.lopezmolina@unige.ch).

A.S. and L.L.-M. conceptualized and designed experiments, and wrote the article; A.S. performed the experiments; U.P. performed the immunoblot experiments; A.S. and G.F. performed and analyzed the electrochromic shift experiments; C.M. performed map-based cloning; L.M.-S. performed fatty acid methyl ester quantification.

[OPEN]Articles can be viewed without a subscription.

www.plantphysiol.org/cgi/doi/10.1104/pp.20.00043

Arabidopsis embryo, as well as that of other oilseed plants, is green and photosynthetically active (Borisjuk and Rolletschek, 2009; Puthur et al., 2013; Allorent et al., 2015). The photosynthetic phase of the embryo starts early upon embryogenesis, at the globular stage, when plastids differentiate into mature chloroplasts and chlorophyll accumulates (Tejos et al., 2010). Overall, embryonic chloroplasts resemble mature chloroplasts in leaves, but they contain less grana with fewer stacks than leaf chloroplasts, possibly as a result of exposure to far-red enriched light within the fruit (Allorent et al., 2015; Liu et al., 2017). As the embryo begins to desiccate, the chloroplasts de-differentiate into nonphotosynthetic plastids, called eoplasts, and the embryo loses its green color, becoming white (Liebers et al., 2017).

The intriguing biological purpose of embryonic photosynthesis remains poorly understood. Indeed, the developing embryo is surrounded by green, photosynthetically active maternal tissues (silique, ovule), which filter the incoming light toward the embryo and render it less suitable for photosynthesis. It has been suggested, in rapeseed (*Brassica napus*), maize (*Zea mays*), and pea (*Pisum sativum*), that embryonic photosynthesis could provide oxygen (O_2) and ATP to cells located in the inner parts of the embryo where it was shown that the concentration of O_2 is limited (Rolletschek et al., 2003; Borisjuk and Rolletschek, 2009; Puthur et al., 2013). Thus, despite its low efficiency, embryonic photosynthesis could favor the developing embryo by supplying necessary oxygen. However, when Arabidopsis developing siliques are kept in the dark, seed development takes place normally, producing viable mature seeds (Kim et al., 2009; Liu et al., 2017). This suggests that embryonic photosynthesis is not essential to produce viable seeds.

Previous reports offer contradictory evidence regarding a potential role of embryonic photosynthesis for food deposition in Arabidopsis mature seeds. Indeed, Liu et al. (2017) observed a decrease in storage reserves when siliques were allowed to develop while wrapped in tinfoil, which blocks light for the developing seeds. However, Allorent et al. (2015) observed that treating developing seeds with 3-(3,4-dichlorophenyl)-1,1-dimethylurea (DCMU), a specific inhibitor of the plastoquinone binding site of PSII, effectively blocks embryonic photosynthesis but does not affect final lipid and protein food stores. In other oilseeds, previous reports suggested that the energetic requirements of the developing seed are fulfilled by the mother plant (Hobbs et al., 2004; Hua et al., 2012). Thus, the role of embryonic photosynthesis for Arabidopsis food storage accumulation remains to be clarified, although in other oilseeds it appears that maternal photosynthesis is sufficient to ensure food deposition.

Embryonic chloroplasts, rather than photosynthesis per se, could play an important role during seed development. Against this hypothesis, some mutants unable to produce functional chloroplasts can still complete seed development. For example, seeds of *plastid protein import2*, which lacks the major plastid protein import receptor TOC159, germinate normally but exhibit seedling lethality due to their inability to produce functional chloroplasts (Tada et al., 2014; Pogson et al., 2015). Yet, the developing embryo invests in what could be regarded as a high energy-consuming process of manufacturing and disassembling chloroplasts.

Available evidence rather suggests that embryonic photosynthesis could play a role after seed maturation. Indeed, previous reports have suggested that embryonic photosynthesis influences seed germination. Interestingly, when developing seeds were treated with DCMU, Allorent et al. (2015) observed that subsequent mature seeds exhibited lower longevity and delayed germination. Genetic experiments, using *ccb2* mutants, which are deficient in the assembly of the cytochrome b6f complex that is essential for photosynthesis, further confirmed that decreased longevity and delayed germination resulted from perturbing embryonic rather than maternal photosynthesis (Allorent et al., 2015).

An unavoidable by-product of photosynthesis is singlet oxygen species ($^1O_2$), which have been implicated in retrograde signaling between the plastid and the nucleus (Nater et al., 2002; Wagner et al., 2004; Lee et al., 2007; op den Camp et al., 2013). In a study focused on the plastid proteins EXECUTER1 (EX1) and EX2, Kim et al. (2009) provided compelling evidence that $^1O_2$-dependent retrograde signaling during seed development is essential for chloroplast development during seedling establishment after seed germination. Indeed, seedlings of the double mutant *ex1 ex2* accumulated less chlorophyll and had smaller chloroplasts compared to wild type. However, when *ex1 ex2* seeds underwent seed development in the dark, both chloroplast development and chlorophyll content in the seedlings were rescued.

In this study, we further explored the role of embryonic photosynthesis for postgerminative plant growth and development, using genetic and pharmacological tools. These include a newly identified temperature-sensitive mutation in *CPN60α2* (AT5G18820), encoding a monomer of the chloroplast chaperoning60 (CPN60) complex, which assists in protein folding in the chloroplast. These tools were used to interfere with the embryonic photosynthetic apparatus, which had profound consequences for postgerminative plant growth and development.

RESULTS

Identification and Characterization of a Temperature-sensitive Photosynthesis-deficient Mutant

In an ethyl methanesulfonate-mutagenesis genetic screen, we identified a recessive mutant, referred to as *ems50-1*, displaying a pale-green phenotype in cotyledons and leaves (Fig. 1A; Supplemental Fig. S1A; see "Materials and Methods"). Interestingly, the pale-green phenotype was observed in plants grown under low temperatures (e.g. 10°C) but not under normal

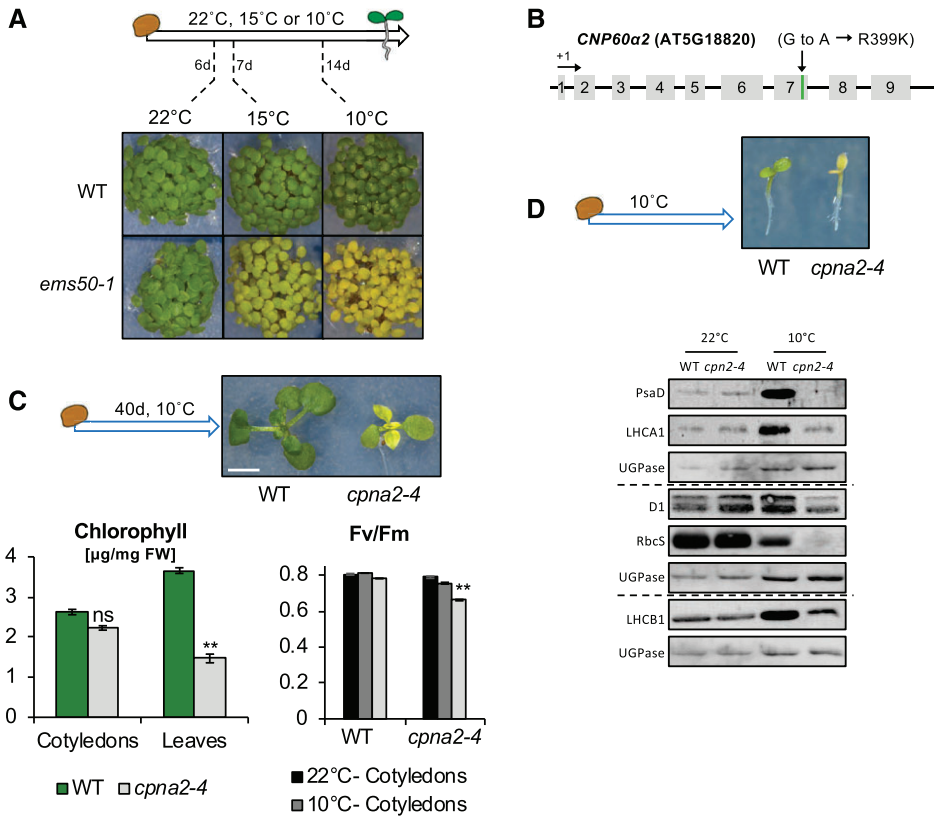

Figure 1. The *cpna2-4* mutant seedlings exhibit a temperature-sensitive phenotype. A, Schematic seedling growth conditions and representative images of wild-type (WT) and *cpna2-4* seedlings at a similar developmental stage after 6, 7, or 14 d of growth at 22°C, 15°C, or 10°C, respectively. B, Genomic structure of *CPN60α2* (AT5G18820). Exons are depicted as gray boxes and the A-to-G mutation causing a R399K amino acid substitution in *cpna2-4* mutants is shown. C, Schematic of seedling growth conditions and representative images of wild-type and *cpna2-4* seedlings after 40 d of growth at 10°C. Scale bar = 4 mm. Bottom left shows total chlorophyll accumulation in cotyledons and newly emerged leaves ($n = 3$). Bottom right shows maximum PSII quantum efficiency (F_v/F_m) in wild-type and *cpna2-4* 40-d–old seedlings grown at 10°C ($n = 6$). Mean ± SE; $^{**}P < 0.01$ with two-tailed *t* test. ns, not significant. D, Schematic of seedling growth conditions and representative images of 10°C-grown seedlings (top). Accumulation of core PSI (PsaD and LHCA1), PSII (D1 and LHCB1), and RbcS proteins in wild-type and *cpna2-4* seedlings grown at 22°C (for 3 d) or 10°C (20 d) until open cotyledons stage (as depicted in the top picture). Proteins extracted from 0.5 mg of fresh material were loaded per lane and UGPase accumulation was used as a loading control. Dashed line separates distinct immunoblot membranes.

temperatures (22°C). This suggested that *ems50-1* is a temperature-sensitive mutation affecting the photosynthetic machinery in the plant.

We reasoned that the cold-induced *ems50-1* phenotype could provide a useful tool to study the role of embryonic photosynthesis for postgerminative plant growth and development. For this purpose, we proceeded to identify the *ems50-1* mutation and investigate whether the cold-induced pale-green phenotype of *ems50-1* mutants indeed reflects a significant perturbation to one or more aspects of photosynthesis in seedlings and developing embryos.

Map-based cloning identified a G-to-A substitution in AT5G18820 (Fig. 1B; see "Materials and Methods"). This mutation causes a single amino acid substitution (R399K) in *CPN60α2*, encoding a subunit of the chaperonin complex CPN60 (Fig. 1B). CPN60α2 was previously shown to localize to the chloroplast and *cpn60α2* null mutations are embryonic-lethal (Ke et al., 2017). The R399K substitution present in *ems50-1* might therefore represent a weak cold-sensitive *cpn60α2* mutant allele. In turn, given that CPN60α2 is a chloroplastic factor, the R399K substitution in *CPN60α2* suggests that it could be the cause of the cold-induced pale phenotype observed in *ems50-1* mutants.

To evaluate this hypothesis, we took advantage of the recessive lethality of null *cpn60α2* mutations present in transfer-DNA (T-DNA) insertion lines (Salk_061417 and Salk_144574). Heterozygous T-DNA insertion plants were pollinated with pollen from homozygous *ems50-1* plants. When germinated at 10°C, the F1 seed progeny produced green and pale-green seedlings at a 1:1 ratio (Table 1; Supplemental Fig. S1B). We therefore conclude that the R399K substitution in *CPN60α2* is responsible for the cold-induced pale phenotype in *ems50-1*. Henceforth, this mutation will be referred to as *cpna2-4*.

Table 1. *Segregation analysis of wild type and lines bearing different mutations in* CPN60α2
Green and pale phenotype was assessed after 10 d of growth at 10°C. het, heterozygous.

Phenotype	Wild Type	*ems50-1*	Salk_144574^{het}	Salk_061417^{het}	Salk_144574^{het} X *ems50-1*	Salk_061417^{het} X *ems50-1*
Progeny	+/+	*ems50-1*/ *ems50-1*	+/+ or +/−	+/+ or +/−	+/ *ems50-1* or −/ *ems50-1*	+/ *ems50-1* or −/ *ems50-1*
Number	156	196	72	105	119	243
Green	100%	0%	100%	100%	54%	51%
Pale	0%	100%	0%	0%	46%	49%

The cold-induced pale-green phenotype displayed by *cpna2-4* mutants strongly suggested that they accumulate less chlorophyll only under low temperatures. Indeed, *cpna2-4* seedlings cultivated at 10°C accumulated significantly lower chlorophyll levels relative to wild-type seedlings (Supplemental Fig. S2A). By contrast, when cultivated at 22°C, chlorophyll accumulation in *cpna2-4* mutant seedlings was comparable to that of the wild type, although mildly delayed (Supplemental Fig. S2B).

Interestingly, after cultivating *cpna2-4* plants for 40 d at 10°C, the oldest leaves gradually lost their pale appearance and became greener, whereas newly emerged leaves exhibited a pale-green phenotype (Fig. 1C). Furthermore, the low chlorophyll content observed in *cpna2-4* seedlings cultivated at 10°C rapidly increased to wild-type levels upon transfer to 22°C (Supplemental Fig. S2C). These observations suggest that chlorophyll accumulation in *cpna2-4* seedlings is not fully prevented under low temperatures.

To further characterize how the *cpna2-4* mutation affects photosynthesis, we assessed the photosynthetic efficiency in *cpna2-4* seedlings using chlorophyll autofluorescence. Wild-type and *cpna2-4* seedlings cultivated at 22°C for 7 d had similar PSII photochemical capacities (F_v/F_m), whereas the quantum yield of PSII in the light (Φ_{PSII}) was slightly higher in *cpna2-4* seedlings (Supplemental Fig. S2B). Similar results were obtained using wild-type and *cpna2-4* plants cultivated at 22°C at the 10-leaf–rosette stage (Supplemental Fig. S3).

When plants were cultivated at 10°C, both F_v/F_m and Φ_{PSII} were significantly lower in 14-d–old *cpna2-4* seedlings compared to wild type (Supplemental Fig. S2A). In wild-type and *cpna2-4* seedlings grown at 10°C for 40 d, F_v/F_m and Φ_{PSII} measured in *cpna2-4* green cotyledons were similar to those measured in wild-type cotyledons, whereas in *cpna2-4* pale leaves, both F_v/F_m and Φ_{PSII} were mildly but significantly lower than in wild-type leaves (Fig. 1C; Supplemental Fig. S4).

We monitored the levels of core PSI and PSII proteins in wild-type and *cpna2-4* seedlings, such as PsaD (PSI), LHCA1 (PSI), D1 (PSII), and LHCB1 (PSII). We also monitored Rubisco small subunit (RbcS). Accumulation of these proteins was significantly lower relative to wild type only in *cpna2-4* seedlings cultivated at 10°C (Fig. 1D).

These data strongly suggest that the *cpna2-4* mutation markedly perturbs photosynthesis under low temperatures. However, over time, *cpna2-4* mutant seedlings are able to develop a normally functional photosynthetic apparatus, at least from the perspective of chlorophyll and photosynthetic efficiency levels.

We next asked whether chlorophyll accumulation or photosynthetic efficiency is affected in *cpna2-4* mutants cultivated at 22°C upon their transfer to 10°C (Fig. 2A). We observed no significant differences in cotyledon chlorophyll accumulation between wild-type and *cpna2-4* after the transfer (Fig. 2B). In addition, cotyledon chlorophyll autofluorescence revealed no difference in either F_v/F_m and Φ_{PSII} between wild type and *cpna2-4* (Fig. 2C; Supplemental Fig. S5). By contrast, and consistent with results above, newly produced leaves in cold-exposed *cpna2-4* were pale and contained less chlorophyll relative to wild type (Fig. 2B). Similar results were obtained using wild-type and *cpna2-4* plants at the 10-leaf–rosette stage upon transfer to 10°C for an additional 7 d (Supplemental Fig. S3).

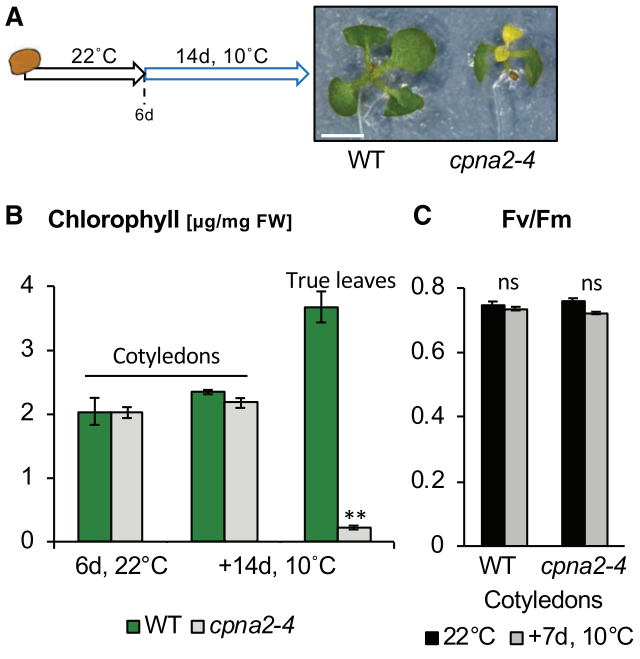

Figure 2. *cpna2-4* mutant seedlings display cold sensitivity only in tissues newly produced under cold conditions. A, Schematic of seedling growth conditions and representative images of wild-type (WT) and *cpna2-4* seedlings grown at 22°C for 6 d followed by an additional 14 d at 10°C. Scale bar = 4 mm. B, Total chlorophyll accumulation in cotyledon and newly emerged true leaves ($n = 3$). C, F_v/F_m in cotyledons 7 d upon transfer to 10°C ($n = 6$). Mean ± SE; $^{**}P < 0.01$ with two-tailed *t* test. ns, not significant.

Altogether, these observations strongly suggest that cold delays the establishment of a fully functional photosynthetic apparatus in *cpna2-4* mutants rather than perturbing the function of a pre-established one.

The *cpna2-4* Mutation Affects Embryonic Photosynthesis in a Cold-induced Manner

We next explored whether the *cpna2-4* mutation affects embryonic photosynthetic activity. First, we measured chlorophyll accumulation in wild-type and *cpna2-4* embryos throughout their development at 22°C (Fig. 3A).

Wild-type embryos were visibly green from the early torpedo stage, consistent with previous results (Fig. 3B; Tejos et al., 2010). Thereupon, the green color intensified until the onset of desiccation, where embryos became white (Fig. 3B). Accordingly, chlorophyll content gradually increased from the torpedo stage, then peaked at the mature-green stage before it decreased again during seed maturation (Fig. 3B). At early stages of their development, *cpna2-4* embryos were mildly paler than wild-type embryos; however, after the late walking-stick stage, differences in green color were no longer visible (Fig. 3B). This pattern was mirrored by chlorophyll accumulation, whereby chlorophyll accumulation in *cpna2-4* seeds was mildly delayed, but the maximal value of chlorophyll content in seeds was similar between both genotypes (Fig. 3B). These results are consistent with our observations in young wild-type and *cpna2-4* seedlings cultivated at 22°C (Supplemental Fig. S2B).

Next, we examined chlorophyll levels in wild-type and *cpna2-4* embryos developing at 10°C (Fig. 3A). Although seed development was normal, it was markedly delayed at 10°C in both wild type and *cpna2-4*, with the process completed in approximately two months instead of 2.5 weeks at 22°C (Fig. 3B). Unlike wild-type embryos developing at 22°C, wild-type embryos appeared green only after reaching the walking-stick stage (Fig. 3B). Moreover, chlorophyll content measured in wild-type embryos as they developed at 10°C showed a decrease in the maximal chlorophyll content achieved compared with wild-type embryos developing at 22°C (Fig. 3B). Interestingly, *cpna2-4* embryos developing at 10°C were visibly paler than their wild-type counterparts throughout their development (Fig. 3B). This was confirmed by chlorophyll accumulation measurements (Fig. 3B).

Concerning photosynthetic efficiency, both F_v/F_m and Φ_{PSII} were similar in wild type and *cpna2-4* developing at 22°C or 10°C (Fig. 3C). We further characterized photosynthetic efficiency through nonphotochemical quenching (NPQ) measurements. Under low-light intensities, i.e. up to 50 $\mu E/m^2/s$, NPQ was similar in wild type and *cpna2-4* developing at 22°C or 10°C. Beyond 100 $\mu E/m^2/s$, NPQ was slightly higher in *cpna2-4* embryos compared with the wild-type embryos developing at 22°C or 10°C (Supplemental Fig. S6A). It should be noted that plants were cultivated under 100 $\mu E/m^2/s$ light intensities so that embryos within siliques and ovular tissues received light intensities lower than 100 $\mu E/m^2/s$.

F_v/F_m, Φ_{PSII}, and NPQ represent relative values informing us about the efficiency of photosynthesis but they do not inform us whether overall photosynthetic activity is affected in *cpna2-4* mutants. To assess the latter, we measured photosynthetic electron flow capacity using the electrochromic shift (ECS) as a proxy (Allorent et al., 2015). The ECS is a modification of the absorption spectrum of specific pigments caused by changes in the transmembrane electric field in the plastid, which in turn reflects changes in the photosynthetic activity (Bailleul et al., 2010). To facilitate the experimental dissection procedure, experiments were performed with seeds rather than embryos as reported in Allorent et al. (2015). Indeed, we verified that chlorophyll accumulated principally in the embryo. Furthermore, Φ_{PSII}, F_v/F_m, and NPQ values in seeds were similar to those in embryos (Supplemental Fig. S7). This shows that seeds can be used instead of embryos to assess embryonic photosynthetic activity.

Seeds at the mature-green stage were exposed to a short saturating pulse for complete photosystem activation. We quantified their photochemistry by measuring the amplitude of the ECS signal in a short time range (500 μs, which corresponds to charge separation) and found that the overall charge separation capacity was reduced in mutants' seeds at 10°C (Fig. 3D; Joliot and Delosme, 1974). We employed the same approach to evaluate the rates of electron flow in the different lines. Photosynthetic rates were evinced from the relaxation kinetics of the ECS signal in the dark, as detailed in "Materials and Methods." We found that, although the charge separation capacity in 10°C-*cpna2-4* mutant embryos was significantly lower than in 10°C wild-type embryos, the overall rate of electron flow was similar (Fig. 3E). This suggests that at 10°C, the amount of photosynthetic complexes is reduced in *cpna2-4*, but that these complexes are fully active in the mutant.

To further test this hypothesis, we monitored D1, LHCA1, LHCB1, PsaD, and RbcS protein levels in wild-type and *cpna2-4* embryos developing at 22°C and 10°C. The results (Fig. 3F) clearly show a reduction in D1, LHCA1, LHCB1, and RbcS protein accumulation specifically in 10°C-*cpna2-4* embryos. Similar results were obtained with embryos dissected at the walking cane stage (Supplemental Fig. S8).

Confocal microscope analysis at the mature-green stage of embryos developing at 22°C revealed that chloroplasts in *cpna2-4* embryos were ~25% smaller relative to those in wild-type embryos (Supplemental Fig. S6B). However, *cpna2-4* embryos exhibited an increase of 15% in chloroplast density compared to wild type (Supplemental Fig. S6B). These results potentially indicate that individual chloroplasts in *cpna2-4* embryos contain less chlorophyll due to their smaller size. However, increased chloroplast density in *cpna2-4* embryos likely explains why wild-type and *cpna2-4*

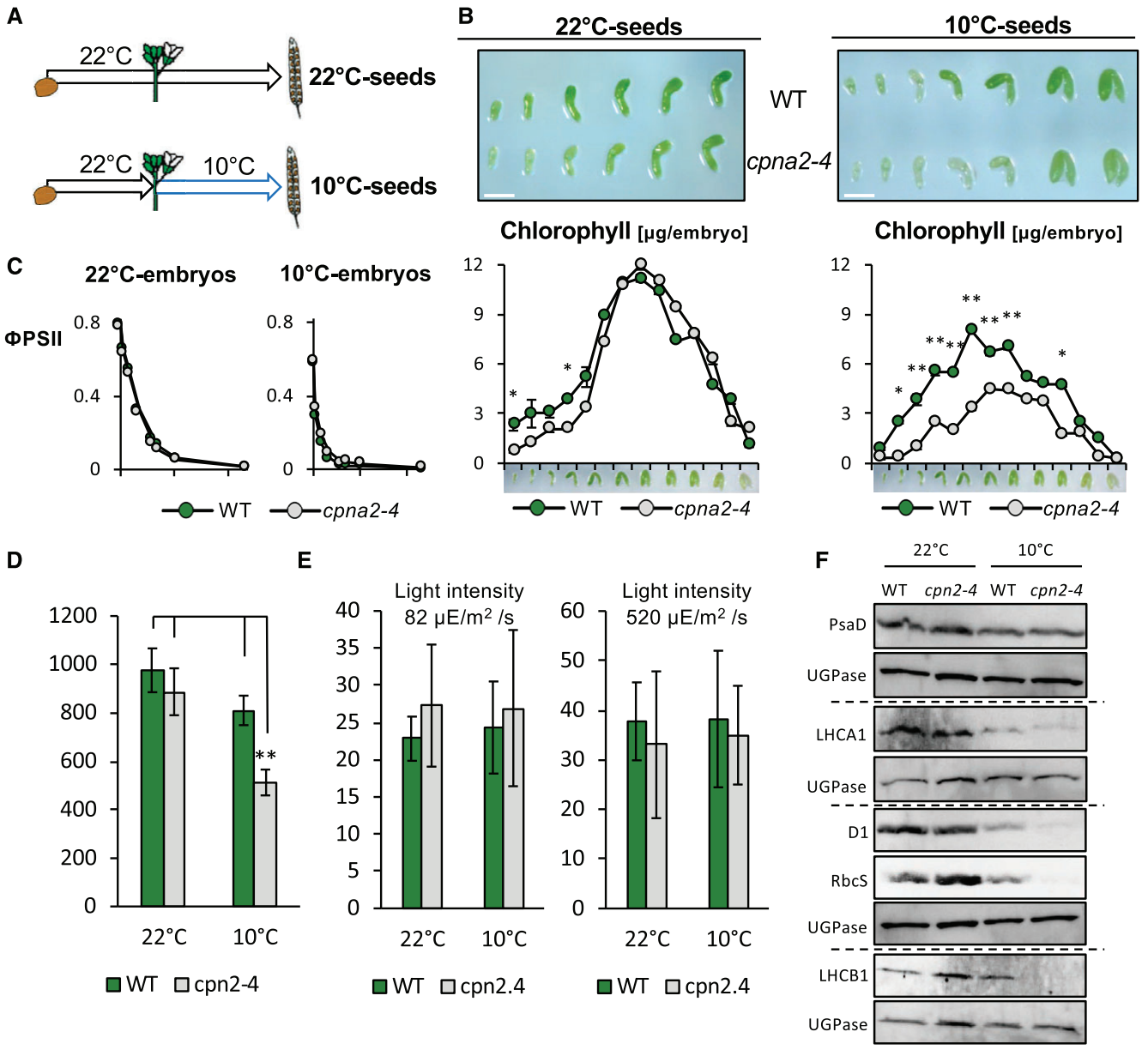

Figure 3. Developing *cpna2-4* mutant seeds accumulate low chlorophyll and core PSI and PSII protein levels under low temperatures. A, Schematic of experimental procedure to produce seeds that developed at 22°C or 10°C. At the time of fertilization, indicated with a flower, plants are either kept at 22°C or transferred to 10°C, as shown. B, Topshows representative images of wild-type (WT) and *cpna2-4* embryos developing at 22°C or 10°C at different developmental stages after fertilization. Scale bar = 0.5 mm. Bottom shows total chlorophyll accumulation throughout wild-type and *cpna2-4* embryo development at 22°C (left) or 10°C (right; $n = 3$). Pictures above graphs show representative embryos for each developmental stage. C, Photosynthetic efficiency (ΦPSII) in mature-green wild-type and *cpna2-4* embryos developing at 22°C or 10°C ($n = 4$). D, In vivo assessment of photochemical capacity via measurements of the ECS. Seeds were exposed to a short (15 μs) saturating light pulse to induce charge separation in all photocenters. This led to a change in the ECS signal that was quantified at 520–546 nm ($n = 3$). E, Quantification of total electron flow of wild-type and mutant seeds. Values represent means ± SE from three biological replicates. Mean ± SE; $^{*}P < 0.05$ and $^{**}P < 0.01$ with two-tailed *t* test. F, Accumulation of core PSI (PsaD and LHCA1), PSII (D1 and LHCB1), and RbcS proteins in embryos of wild-type and *cpna2-4* maturing at 22°C or 10°C. Proteins extracted from 20 embryos were loaded per lane and UGPase accumulation was used as a loading control. Dashed line separates distinct immunoblot membranes.

embryos accumulate similar chlorophyll levels at the mature-green stage at 22°C.

Interestingly, the same analysis in embryos developing at 10°C revealed that chloroplast size in *cpna2-4* embryos further decreased to ~40% of that of wild-type embryos (Supplemental Fig. S6B). However, chloroplast density in *cpna2-4* embryos was only 20% higher relative to that in wild-type embryos (Supplemental Fig. S6B). Thus, these observations suggest that *cpna2-4* embryos, despite their increased chloroplast density, fail to fully compensate for lower chlorophyll levels in individual chloroplasts.

Overall, these data strongly suggest that the photosynthetic apparatus functions properly in *cpna2-4* seeds developing at 22°C whereas exposure to cold decreases photosynthetic activity. We therefore used the *cpna2-4* mutation as a tool to investigate the impact of embryonic photosynthesis for future plant vegetative development.

Embryonic Photosynthesis Affects Subsequent Mature Plant Growth and Development Without Affecting Mature Seed Physiology

Hereafter, wild-type and *cpna2-4* seeds produced as described above at 22°C are referred to as "22°C-wild-type" and "22°C-*cpna2-4*" seeds, respectively, and when produced at 10°C they are referred to as "10°C-wild-type" and "10°C-*cpna2-4*" seeds, respectively (Fig. 3A).

Whereas seed size and weight were similar in wild-type and *cpna2-4* seeds, overall fatty acid content was slightly lower (~10% to 15%) in *cpna2-4* seeds relative to wild-type seeds irrespective of the temperature during seed development; however, this difference was not statistically different (Fig. 4A; Supplemental Fig. S9). Cold during seed development similarly diminished seed size, weight, lipid content, and germination percentage by ~15% in both wild-type and *cpna2-4* seeds, which was statistically significant. However, cold appears to effect seed properties in both genotypes similarly (Fig. 4A; Supplemental Fig. S10).

Given that the *cpna2-4* embryonic photosynthetic apparatus is mainly affected by cold, we conclude that the possible mildly lower seed size, weight, and fatty acid content of *cpna2-4* mutant seeds are unrelated to embryonic photosynthesis. That embryonic photosynthesis does not interfere with lipid content is consistent with previous reports (Allorent et al., 2015).

Next, we studied the impact of embryonic photosynthesis in early postembryonic skoto- and photomorphogenic development.

In the absence of light, hypocotyl and root growth in 22°C-*cpna2-4* seedlings were mildly inhibited compared to that of 22°C-wild-type seedlings. Strikingly, hypocotyl and root growth of 10°C-*cpna2-4* seedlings were markedly inhibited relative to those of 22°C-*cpna2-4* seedlings (Fig. 5A). Interestingly, hypocotyl and root growth in 10°C-wild-type seedlings was mildly, but significantly, inhibited relative to that of 22°C-wild-type seedlings (Fig. 5A; see Discussion below).

In the presence of light, 22°C-*cpna2-4* seedling root growth and cotyledon surface area was mildly but significantly inhibited compared to 22°C-wild-type seedlings. Strikingly, 10°C-*cpna2-4* seedling root growth, hypocotyl length, and cotyledon surface area were all markedly inhibited relative to 22°C-*cpna2-4* seedlings (Fig. 5B). Similarly, as above, 10°C-wild-type seedling root growth and cotyledon surface area were mildly, but significantly, inhibited relative to that of 22°C-wild-type seedlings (Fig. 5B; see "Discussion" below).

We next asked whether the strong early developmental defects of 10°C-*cpna2-4* seedlings could be overcome over time in adult plants. Seven-d–old seedlings were transferred to soil and both the number of leaves and rosette surface area were quantified over time.

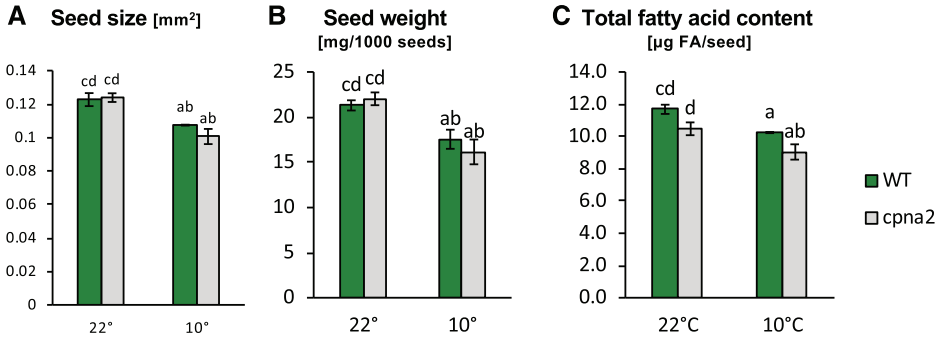

Figure 4. Effect of cold during seed development on wild-type (WT) and *cpna2-4* seed size, weight, and lipid content. A, Wild-type and *cpna2-4* seed size. B, Wild-type and *cpna2-4* seed weight. C, Total fatty acid content in wild-type and *cpna2-4* seeds. The letters "a," "b," "c," and "d" above the bars refer to 22°C-wild type, 22°C-*cpna2-4*, 10°C-wild type, and 10°C-*cpna2-4* plant material, respectively. The presence of a letter above a given bar means that its value is significantly different ($P < 0.05$, two-tailed *t* test) compared to the data associated with the letter. The absence of a letter above a given bar means that there are no statistically significant differences involved. For example, in (A), the bar representing the size of 22°C-wild-type seeds has letters c and d above, indicating that the bar size value is significantly different than the size of 10°C-wild-type (c) and 10°C-*cpna2-4* (d) seeds. Mean ± SE, $n = 3$.

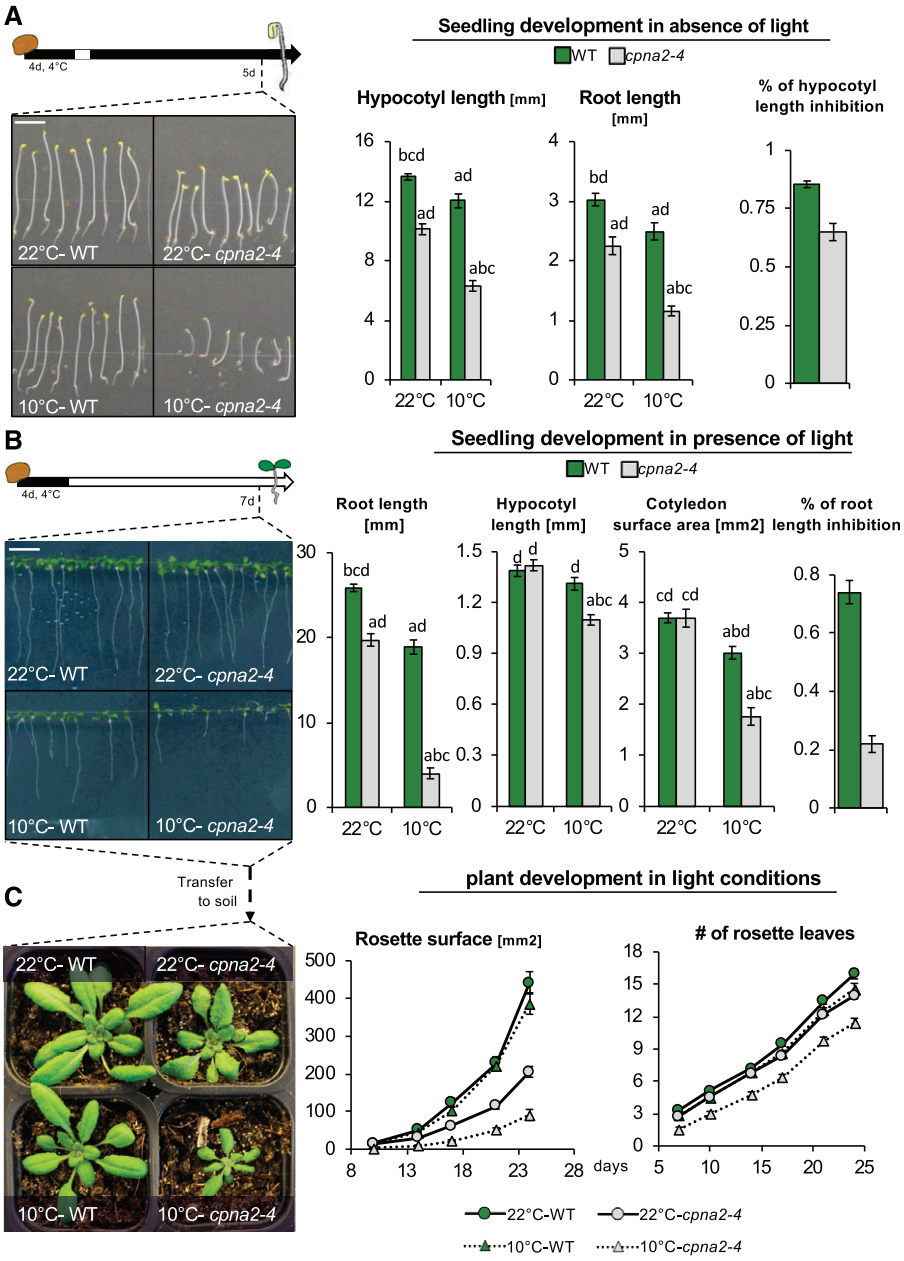

Figure 5. Perturbation of embryonic photosynthesis interferes with juvenile and adult plant development. A, Analysis of 22°C-wild-type (WT), 10°C-wild-type, 22°C-*cpna2-4*, and 10°C-*cpna2-4* early seedling development in the absence of light. Schematic of seedling growth conditions and images of seedlings grown in darkness for 5 d after stratification (left). Scale bar = 5 mm. Histograms showing hypocotyl length, root length, and ratio of 10°C-seedling/22°C-seedling hypocotyl length (right). B, Analysis of 22°C-wild-type, 10°C-wild-type, 22°C-*cpna2-4*, and 10°C-*cpna2-4* seedling development in the presence of light. Schematic of seedling growth conditions and images of seedlings grown in darkness for 7 d after stratification (left). Scale bar = 6 mm. Histograms showing root length, hypocotyl length, cotyledon surface area, and ratio of 10°C-seedling/22°C-seedling root length (right). C, Analysis of 22°C-wild-type, 10°C-wild-type, 22°C-*cpna2-4*, and 10°C-*cpna2-4* plant growth over time. Images of plants grown in soil for 21 d (left). Graphs showing increases in leaf number and rosette surface area over time (right). Mean ± SE, n = 15–20; statistical analysis and nomenclature are as in Figure 4.

Strikingly, the surface area of 10°C-*cpna2-4* rosettes was strongly reduced compared to 22°C-*cpna2-4* rosettes (Fig. 5C). In addition, the number of leaves in 10°C-*cpna2-4* rosettes over time was significantly lower than that of 22°C-*cpna2-4* rosettes. By contrast, no significant differences in any of the above attributes were observed between 22°C-wild-type and 10°C-wild-type plants (Fig. 5C). However, no hypersensitive response to cold during seed development was observed through analysis of *cpna2-4* flowering time (Supplemental Fig. S11). In addition, seed yield was unaffected by cold during seed development in both wild type and *cpna2-4* (Supplemental Fig. S11).

All together, these observations strongly suggest that perturbing the embryonic photosynthetic apparatus leads to profound developmental defects starting from early postembryonic seedling development and well into the vegetative phase of the plant. However, our results indicate that flowering time and seed yield are not compromised.

Cold-induced Developmental Defects Are Unrelated to the Maternal Genotype

In the above experiments, mother *cpna2-4* plants were exposed to cold after bolting. Given that cold exposure does not significantly alter photosynthetic activity in pre-existing *cpna2-4* leaves, the observed seedling developmental defects are unlikely to result from the *cpna2-4* maternal genotype. To further test this

possibility, we pollinated *cpna2-4* heterozygous (*cpna2-4/+*) plants with *cpna2-4* mutant pollen (from *cpna2-4/cpna2-4* plants), producing *cpna2-4/cpna2-4* or *+/cpna2-4* seeds (Fig. 6A). Consistent with results above, *cpna2-4/cpna2-4* accumulated less chlorophyll as well as lower levels of D1, LHCA1, LHCB1, and RbcS relative to *+/cpna2-4* embryos developing at 10°C (Fig. 6, B and C). As expected, only 10°C-*cpna2-4/cpna2-4* seeds produced seedlings with developmental defects as assessed by measuring root length in 7-d–old seedlings (Fig. 6D). We also pollinated *cpna2-4* plants with wild-type pollen, which yields phenotypically wild-type *cpna2-4/+* seeds (Supplemental Fig. S12). The resulting 10°C-*cpna2-4/+* seedlings displayed a postgermination development similar to that of 10°C-wild-type seedlings (Supplemental Fig. S12).

Hence, these results show that the seedling developmental defects induced by cold during *cpna2-4* seed development reflect the effect of cold in fertilization tissues only. These results further support the conclusion that embryonic photosynthetic activity is essential for normal seedling development.

Cold Applied to Photosynthetically Active *cpna2-4* Embryos Does Not Induce Developmental Defects

The observed developmental defects observed in *cpna2-4* plants could be due to the effect of cold in developing *cpna2-4* embryos in a manner unrelated to their lower photosynthetic activity. To address this possibility, we took advantage of the fact that cold does not significantly perturb previously established photosynthetic activity (Supplemental Fig. S13). In this experiment, wild-type and *cpna2-4* seed development was allowed to proceed at 22°C until the late walking-stick stage (10 d after fertilization [DAF]), when both wild-type and *cpna2-4* embryos are photosynthetically active, and were then transferred to 10°C to complete their development. These seeds are referred to as "10°C-10 DAF" seeds (Fig. 7A).

When germinated, both 10°C-10 DAF wild-type and *cpna2-4* seedlings developed normally in the presence of light (Fig. 7B), showing that a cold treatment that does not lower photosynthetic capacity in *cpna2-4* embryos does not affect future seedling growth.

We further assessed whether a short cold exposure could affect future seedling growth. For this purpose, developing seeds of both wild-type and *cpna2-4* were exposed to 10°C for 14 d, staring at 0 DAF or 10 DAF, referred to as "early-10°C-wild-type" or "early-10°C-*cpna2-4*" seedlings, and "late-10°C-wild-type" or "late-10°C-*cpna2-4*" seedlings, respectively (Supplemental Fig. S14A). In accordance with previous results, both late-10°C-wild-type and late-10°C-*cpna2-4* seedlings developed normally in the presence of light (Supplemental Fig. S14B). However, early-10°C-*cpna2-4* seedlings exhibited developmental defects that were more pronounced than

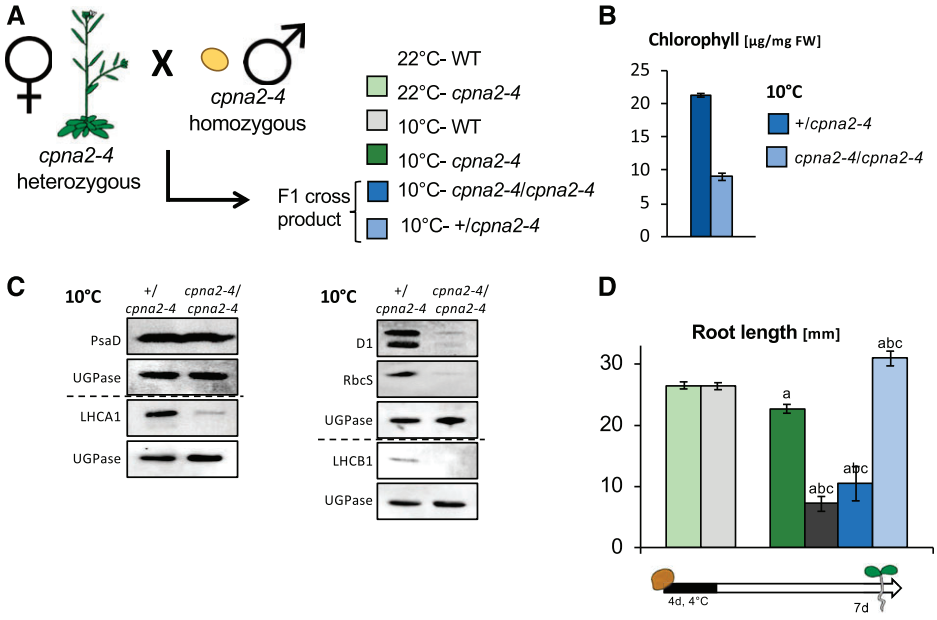

Figure 6. Cold-induced developmental defects are unrelated to the maternal genotype. A, Schematic of the cross performed by pollinating *cpna2-4/+* plants with *cpna2-4* pollen. The seeds from this cross were allowed to develop at 10°C. B, Total chlorophyll accumulation in mature-green seeds developing at 10°C. C, Accumulation of core PSI (PsaD and LHCA1), PSII (D1 and LHCB1), and RbcS proteins in *cpna2-4/+* and *cpna2-4/cpna2-4* embryos maturing at 10°C obtained as described in (A). Pale-green embryos (genotype *cpna2-4/cpna2-4*) were separated from wild-type (WT)–like green embryos (genotype *cpna2-4/+*) from the same siliques. Proteins extracted from 20 embryos were loaded per lane and UGPase accumulation was used as a loading control. Dashed line separates distinct immunoblot membranes. D, Schematic of seedling growth conditions (bottom) and histogram showing root length of seedlings in the presence of light. Mean ± SE, $n = 12–20$; statistical analysis and nomenclature are as in Figure 4. FW, fresh weight.

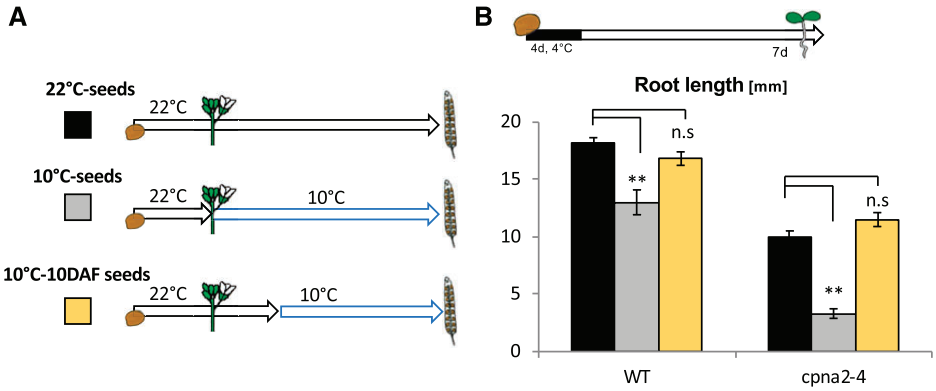

Figure 7. Cold applied to photosynthetically active *cpna2-4* embryos does not induce developmental defects. A, Schematic of experimental procedure to expose developing seeds to cold at different stages of their development; wild-type (WT) and *cpna2-4* seeds were allowed to develop at 22°C, or were exposed to 10°C starting at either 0 or 10 DAF (22°C-seeds, 10°C-seeds, and 10°C-10DAF seeds, respectively). B, Schematic of seedling growth conditions (top) and histogram showing seedling root length 7 d after seed stratification in the presence of light. Mean ± SE, $n = 15–22$; $^{**}P < 0.01$ with two-tailed *t* test. ns, not significant. WT, wild type.

in early-10°C-wild-type seedlings. Interestingly, these defects were milder relative to those exhibited by 10°C-*cpna2-4* seedlings (Supplemental Fig. S14B). This suggests that a short-lasting perturbation of embryonic photosynthesis is sufficient to cause seedling developmental defects, which is more severe when photosynthesis is perturbed for a longer period. We also observed that early-10°C-wild-type seedling development was mildly affected when compared to that of 22°C-wild-type seedlings (see "Discussion").

Taken together, these observations further support the notion that perturbation of photosynthesis in developing *cpna2-4* seeds, rather than cold exposure, is the cause of the developmental defects observed in 10°C-*cpna2-4* seedlings.

To further test this notion, we used independent genetic and pharmacological approaches.

cpna1-2 Is A Temperature-sensitive Mutation that Phenocopies *cpna2-4*

CPN60α2 and *CPN60α1* encode close homologs whose tertiary structure is predicted to be very similar (Vitlin Gruber et al., 2018). A *cpna1-2* allele was mistakenly reported to cause a D335A substitution (Peng et al., 2011). Instead, we found that it causes a D335N substitution (see "Materials and Methods"). We noticed that the D335N substitution induced by the *cpna1-2* allele affects the same location as that of the *cpna2-4* allele within the predicted respective CPN60α1 and CPN60α2 three-dimensional structures (Supplemental Fig. S15).

Interestingly, we observed that *cpna1-2* seedlings also displayed a pale phenotype when cultivated in cold (Supplemental Fig. S15). Furthermore, 22°C-*cpna1-2* seedling growth was mildly but significantly inhibited compared to 22°C-wild-type seedlings. Strikingly, 10°C-*cpna1-2* seedling development was markedly defective in comparison to that of 10°C-wild-type seedlings (Fig. 8A). We therefore conclude that the *cpna1-2* mutation provides independent genetic confirmation for our observations with *cpna2-4* mutants.

toc159 Mutants Have Abnormal Skotomorphogenic Development

TOC159 encodes an essential component of the preprotein import machinery at the outer chloroplast membrane and is therefore essential for chloroplast biogenesis (Tada et al., 2014). *toc159* mutants are not viable; however, *toc159* mutant seeds developing in a *toc159*/+ heterozygous mother plant can complete their development, and germinate normally. We found that *toc159* mutants produced by 22°C-*toc159*/+ mother plants had skotomorphogenic defects similar to those observed with 10°C-*cpna2-4*seedlings (Fig. 8B, Supplemental Fig. S16). We further tested additional mutants reported to be albino or defective in chloroplast development, such as *hmr2*, *pac*, *skl1*, and *cp33a-1*, using heterozygous mother plants (Holding et al., 2000; Chen et al., 2010; Teubner et al., 2017). In all mutants tested, we observed similar results to those observed using *toc159*: skotomorphogenic growth in mutant seedlings was defective compared to that of heterozygous and wild-type seeds from the same segregating progeny population (Supplemental Fig. S16). These observations further support the conclusion that embryonic photosynthetic activity is essential for normal seedling development.

DCMU-treated Developing Seeds Produce Seedlings with Developmental Defects

DCMU specifically inhibits photosynthesis by blocking the plastoquinone binding site of PSII, which disrupts electron flow. Developing siliques of Col-0 were painted with a 1-mM DCMU solution at 5, 8, 10, 13, and 15 DAF and developing seeds were allowed to mature

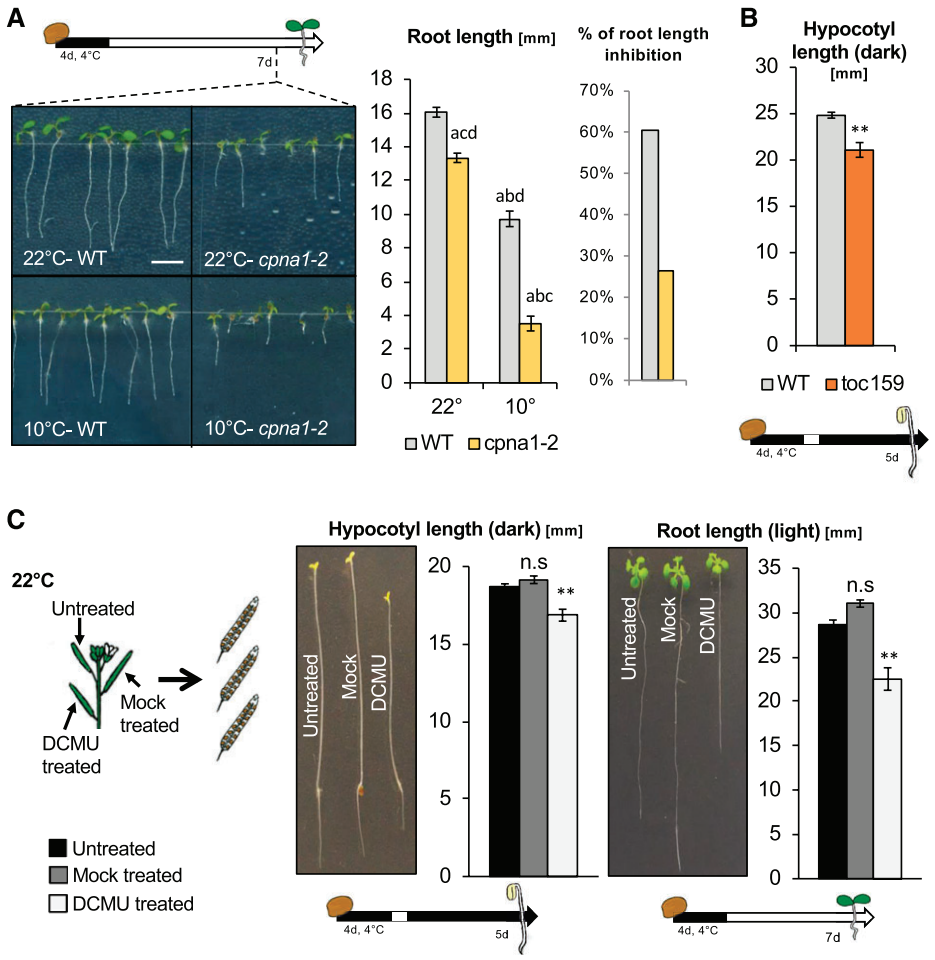

Figure 8. *cpna1-2* is a temperature-sensitive chloroplast chaperonin, which phenocopies *cpna2-4*; *toc159* mutants display abnormal skotomorphogenic development; and DCMU-treated developing seeds produce seedlings with developmental defects. A, Schematic of seedling growth conditions (top left) and representative images of 7-d–old wild-type (WT) and *cpna1-2* light-grown seedlings arising from seeds that developed at either 22°C or 10°C. Scale bar = 5 mm. Histograms showing root length and ratio of 10°C-seedling/22°C seedling root length (right). Statistical analysis and nomenclature as in Figure 4. B, Schematic of seedling growth conditions (bottom) and histogram showing hypocotyl length of wild-type and *toc159* seedlings grown in the absence of light for 5 d. C, Schematic (left) shows experimental procedure to produce seeds treated with DCMU. Representative images of dark- and light-grown seedlings (middle and right) arising from treated (DCMU) or untreated (Untreated, Mock) seeds. Schematics of seedling growth conditions are provided below. Histograms show quantification of seedling hypocotyl and root length. Mean ± SE, $n = 15–22$; $^{**}P < 0.01$ with two-tailed *t* test. ns, not significant.

(Fig. 8C). Consistent with previous reports, DCMU treatment fully disrupted photosynthesis in developing embryos (Supplemental Fig. S17A; Allorent et al., 2015).

After stratification, DCMU-wild-type seed germination frequency was similar to that of control seeds (Supplemental Fig. S17B). However, DCMU-wild-type seedlings exhibited abnormal skotomorphogenesis, similar to that observed with 10°C-*cpna2-4* seedlings; i.e. they had short hypocotyls and roots (Fig. 8C). Similarly, in the presence of light, DCMU-wild-type seedling root and vegetative growth was strongly inhibited (Fig. 8C). Similar results were obtained with different Arabidopsis accessions (C24, Landsberg *erecta*, Cape Verde Islands, and Wassilewskija [Ws]; Supplemental Fig. S17C).

These observations provide independent pharmacological evidence that embryonic photosynthesis is essential for normal postgermination seedling development.

Seedling Developmental Defects Are Not Associated with Defective Photosynthesis

We then proceeded to explore the possible underlying reason for the observed developmental defects in 10°C-*cpna2-4* plants. Our analysis of the mature dry seed indicated that perturbing embryonic photosynthesis did not affect seed food stores, consistent with previous reports using DCMU-treated seeds (Fig. 4; Allorent et al., 2015). This observation, combined with the observation that 10°C-*cpna2-4* plants retained developmental defects when fully engaged in the vegetative phase of their life cycle, further suggests that food storage in 10°C-*cpna2-4* seeds is not the underlying cause for the 10°C-*cpna2-4* seedling developmental defects. Consistent with this notion, the developmental defects of 10°C-*cpna2-4* seedlings were not rescued by exogenous Suc (Fig. 9A).

Developmental defects could reflect a defect in the photosynthetic apparatus in 10°C-*cpna2-4* seedlings. However, confocal analysis did not reveal considerable alterations in chloroplast size or density in 10°C-*cpna2-4* seedlings (Fig. 9B). Furthermore, no significant perturbations in chlorophyll content nor in photosynthesis efficiency were detected in 10- or 25-d–old 10°C-*cpna2-4* plants (Fig. 9B).

These observations indicate that impaired photosynthesis in the seedling is not the underlying cause of the developmental defects of 10°C-*cpna2-4* plants.

DISCUSSION

The *cpna2-4* Mutant Allele Provides a Novel Tool To Study the Role of Embryonic Photosynthesis

We here identified *cpna2-4*, a new viable allele of the chloroplast chaperonin subunit CPN60α2 (AT5G18820). We show that, relative to wild type, *cpna2-4* chlorophyll accumulation is markedly reduced in both vegetative and embryonic tissues only when *cpna2-4* mutants are exposed to 10°C. However, we did not detect differences in photosynthetic efficiency when comparing wild-type and *cpna2-4* mutant seeds developing at 22°C and 10°C. Furthermore, we provide evidence that in *cpna2-4* mutants cold delays the establishment of a fully functional photosynthetic apparatus rather than perturbing the function of a pre-established one. Altogether, given that this mutant accumulates lower amounts of photosynthetic pigments and complexes at low temperature, the *cpna2-4* mutation provides a tool to reduce either vegetative or embryonic photosynthesis in cold-dependent manner. Thus, the *cpna2-4* mutant allele allows the specific manipulation of embryonic photosynthesis in a temperature-dependent manner, providing a new tool to study its biological role. However, it should be noted that 22°C-*cpna2-4* seedlings have mild development defects despite the absence of major photosynthetic defects in *cpna2-4* mutants. Furthermore, DCMU-treated developing seeds produced seedlings with developmental defects that were milder than those of 10°C-*cpna2-4* seedlings. This suggests that CPN60 activity in embryonic chloroplasts could additionally induce future seedling growth defects by perturbing chloroplastic function independently of photosynthesis. However, our data show that cold must induce these defects only in the context of disrupted photosynthesis. Indeed, when *cpna2-4* embryos are completely photosynthetically active, wherein exposure to cold does not disrupt photosynthesis, *cpna2-4* seedling development is not affected by the cold treatment during embryogenesis (Supplemental Fig. S13). This shows that a mere exposure of *cpna2-4* embryos to cold is not sufficient to strongly disrupt future seedling development. To date, only very few of the protein targets of CPN60 have been identified. While other chloroplast functions may be perturbed in *cpna2-4* mutants exposed to cold, further research is needed to identify these. In the scope of this research we have focused on the perturbation of photosynthesis and its effect on future seedling development.

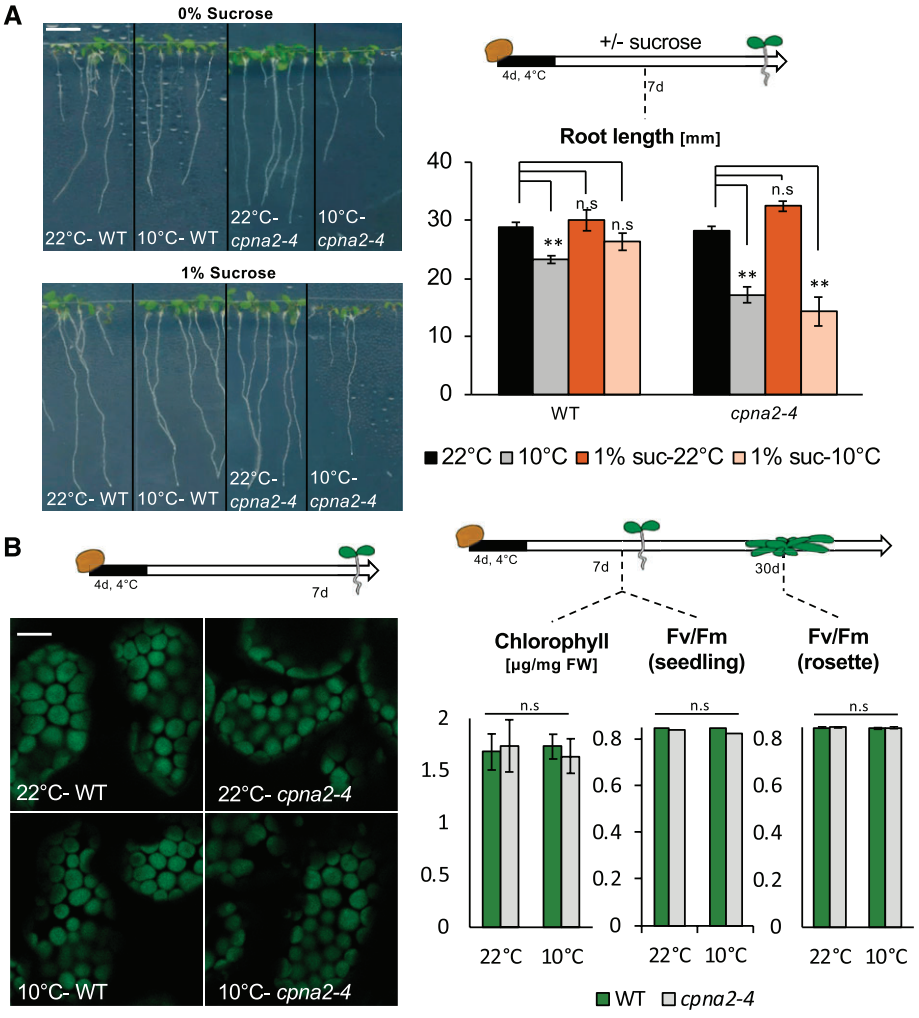

Figure 9. Seedling developmental defects are not corrected by exogenous Suc nor are they associated with defective photosynthesis. A, Representative images of seedlings (left) cultivated in the presence of light for 7 d after seed stratification in the absence (0%) or presence (1%) of Suc. Scale bar = 6 mm. Schematic (right) of seedling growth conditions and histogram showing root length quantification of 7-d–old 22°C-wild-type (WT), 10°C-wild-type, 22°C-*cpna2-4*, and 10°C-*cpna2-4* seedlings grown in media with or without 1% Suc (n = 15–25). B, Schematic of seedling growth conditions (top left) and confocal microscope images (bottom left) of cotyledon chloroplasts of 7-d–old 22°C-wild-type, 10°C-wild-type, 22°C-*cpna2-4*, and 10°C-*cpna2-4* seedlings. Green coloring is chlorophyll autofluorescence. Scale bar = 4 µm. Schematic of plant growth conditions (top right) and histograms (bottom right) showing total chlorophyll accumulation in 7-d–old 22°C-wild-type, 10°C-wild-type, 22°C-*cpna2-4*, and 10°C-*cpna2-4* light-grown seedlings and maximum PSII quantum efficiency (F_v/F_m) in 7-d–old seedlings or 30-d–old mature rosettes, as indicated (n = 5–6). Mean × SE. ns, not significant.

Embryonic Photosynthesis Plays a Profound Role for Future Plant Development

Using the *cpna2-4* mutation, in combination with orthogonal genetic and pharmacological approaches, we show that altering embryonic photosynthesis leads to defects in early postembryonic development in both the presence and absence of light, as well as in long-term adult plant development (Fig. 5). Furthermore, we were able to show that maternal photosynthesis does not participate in the observed developmental defects (Fig. 6).

These observations provide strong evidence that embryonic photosynthesis plays a profound role in priming the future growth of the plant.

It could be argued that the genetic approaches using the *cpna2-4*, *cpna1-2*, and *toc159* mutants induce developmental defects due to pleiotropic effects relating to chloroplast function rather than to reduced photosynthetic activity. To address this possibility, we employed DCMU-treated seeds, which also produced seedlings exhibiting developmental defects in both skoto- and photomorphogenic light conditions. These experiments therefore provide evidence of a direct link between photosynthesis during seed development and future seedling growth. However, additional chloroplast functions during embryogenesis that may be consequential for future postgerminative development cannot be ruled out.

Possible Roles of Embryonic Photosynthesis

It Remains To Be Understood How Embryonic Photosynthesis Affects Future Plant Development

Allorent et al. (2015) reported that treating developing seeds with DCMU did not affect food stores in seeds. By contrast, Liu et al. (2017) reported that seeds that develop in the absence of light fail to accumulate lipid bodies. Our data support the results obtained by Allorent et al. (2015; Fig. 4). Furthermore, low food deposition in seeds is expected to be consequential only for early postgerminative growth. We therefore tend to exclude a role of seed food storage to explain the developmental defects reported here.

Allorent et al. (2015) reported modest changes (<2-fold) in the levels of a restricted number of metabolites in seeds after DCMU treatment. These include higher GABA and lower galactinol and Pro levels in DCMU-treated seeds relative to untreated controls. Concerning GABA, Allorent et al. (2015) argued that higher GABA levels could result from a state of anoxia in the embryo of DCMU-treated seeds. This is consistent with the notion that embryonic photosynthesis could provide oxygen to embryonic tissues to facilitate their development (Borisjuk and Rolletschek, 2009). Galactinol and Pro are osmoprotectants expected to scavenge ROS and maintain protein folding during dehydration. This led Allorent et al. (2015) to propose that embryonic photosynthesis is involved for proper seed desiccation and longevity. These arguments were introduced to account for the seed physiological defects observed by Allorent et al. (2015) as a result of treating developing seeds with DCMU (slower seed germination, reduced longevity). However, tissue damage induced by anoxia or protein misfolding resulting from lower osmoprotectants in seeds does not provide an obvious explanation for the developmental defects in seedling and adult plant development reported here.

We showed that perturbing embryonic photosynthesis does not result in deficient photosynthesis, chlorophyll content, and chloroplast morphology in seedlings, which is consistent with results obtained by Allorent et al. (2015) examining photosynthesis in 7-d–old seedlings obtained from DCMU-treated seeds. Furthermore, the skotomorphogenic defects of seedlings arising from photosynthetically deficient seeds exclude the possibility of impaired photosynthesis as the underlying cause for these defects. Thus, altered photosynthesis in the seedling does not readily explain the developmental defects in seedlings and adult plants reported here.

Nevertheless, this does not exclude the possibility that the observed developmental defects are because photosynthetically deficient embryos produce plants with deficient chloroplasts. Indeed, chloroplasts are directly or indirectly involved in numerous, if not all, cellular and developmental processes in plants, including those pertaining to hormone synthesis (Chan et al., 2016). A deficient chloroplast function is therefore an attractive hypothesis accounting for our observations. This hypothesis implies that photosynthetically active embryonic chloroplasts are required for their proper de-differentiation into eoplasts during seed maturation. As a result, developmentally defective eoplasts may lead to long-lasting defects in chloroplast development and function in vegetative tissues. This hypothesis is consistent with the results obtained by Kim et al. (2009), suggesting that retrograde signaling activated by $^1O_2$ emanating from embryonic photosynthesis is important for eoplast differentiation into chloroplasts during seedling establishment. Further testing of this hypothesis requires an in-depth investigation of chloroplastic function in plants arising from photosynthetically deficient seeds.

During the vegetative phase of the plant life cycle, the chloroplast is known to play a prominent role in abiotic stress responses—in particular, chilling stress (Crosatti et al., 2013; Liu et al., 2018). Interestingly, wild-type seeds that developed under cold temperatures accumulated lower chlorophyll levels and this correlated with a mild developmental delay in wild-type seedlings (Fig. 3). We speculate that embryonic chloroplasts could play a role in the embryonic chilling response, which is associated with a decrease in chlorophyll levels and photosynthetic complexes (Fig. 3). In turn, this may also interfere with proper de-differentiation into eoplasts, which could account for the observed mild lasting effects on plant development (Fig. 4). This is consistent with the results obtained with *cpna2-4*

mutants, where exposure to cold leads to an exacerbated decrease in chlorophyll levels and severe, long-lasting developmental defects in plants.

Lastly, recent studies have shown that exposure to cold during seed development leads to epigenetic changes in the embryo (Iwasaki et al., 2019). This could suggest that perturbing embryonic photosynthesis may interfere with normal epigenetic mark deposition in embryos, resulting in long-lasting developmental defects in the progeny.

CONCLUSION

The biological purpose of embryonic photosynthesis has not been extensively investigated and is poorly understood. A few studies have attempted to understand the role of embryonic photosynthesis by experimentally interfering with it. These reports were mainly concerned with investigating the consequences of perturbing embryonic photosynthesis on seed physiology, germination, and the onset of chloroplast development during seedling establishment (Kim et al., 2009; Allorent et al., 2015; Liu et al., 2017). Whether perturbing embryonic photosynthesis has long-lasting effects in future plant development, growth, and health was not investigated. In this work, we further expanded on this line of research. Using different genetic and pharmacological approaches, we show that embryonic photosynthesis plays a profound role in determining the future growth and development of the plant.

MATERIALS AND METHODS

Statistical Analysis

Significant values were determined using the Student's *t* test, with $P < 0.05$, $P < 0.01$. All data were analyzed with at least three biological replicates.

Plant Materials

Arabidopsis (*Arabidopsis thaliana*) lines used in this study were primarily in the Columbia (Col-0) background, unless otherwise stated. Additional Arabidopsis accessions used: C24, Cape Verde Islands, Ws, and Landsberg *erecta*.

The following Arabidopsis T-DNA insertion mutant seeds were obtained from the Nottingham Arabidopsis Stock Center (Scholl et al., 2000): Salk_061417, Salk_144574, Salk_025099, Salk_080596, and Salk_121656.

The *cpna1-2* seeds were kindly provided by Toshiharu Shikanai (Peng et al., 2011). *toc159* seeds were kindly provided by Felix Kessler (Shanmugabalaji et al., 2018). The *cp33a-1* seeds were kindly provided by Christian Schmitz-Linneweber (Teubner et al., 2017)

Plant Growth Conditions

Arabidopsis plants were grown under the following conditions: 22°C, 100 $\mu E/m^2/s$ white light, 16-h light:8-h dark, 70% relative humidity. To produce 10°C seeds, plants were grown as described above until 4–6 inflorescences were detectable. Flowers were marked at the time of fertilization and plants were transferred to cold conditions (10°C, 100 $\mu E/m^2/s$ white light, 16-h light:8-h dark, 70% relative humidity) for the duration of seed development. Afterward, seeds were after-ripened at room temperature for one week, then stored at −80°C.

For use in germination tests and early seedling development assays, seeds were surface-sterilized (one-third bleach, two-thirds water, and 0.05% Tween), followed by three washes in double-distilled water, and germinated on Murashige and Skoog medium (4.3 g/L) with MES (0.5 g/L) and 0.8% (w/v) Bacto-Agar (Applichem). Plates were incubated at a given temperature, under 80 $\mu E/m^2/s$, 16-h light:8-h dark, 70% relative humidity.

To prepare DCMU-treated seeds, plants were grown under 22°C growth conditions and siliques were painted at 5, 8, 10, 13, and 15 DAF with 1-mM DCMU in 0.1% Tween 20 (w/v; DCMU-treated samples) or with 0.1% Tween 20 (w/v; control treatment). The detergent enhances inhibitor diffusion through the cuticle (Allorent et al., 2015).

Mutant Screening, Molecular Mapping, and Whole-genome Sequencing

With the aim of identifying mutants displaying abnormal postembryonic development in low temperatures, a previously establish population of ethyl methanesulfonate-treated seeds were used (M1; Kim Woohyun et al., 2019). M2 seeds were germinated at 10°C, and screened for abnormal phenotypes.

For map-based cloning and whole-genome sequencing, the *ems50-1* mutants were outcrossed to Ws. The respective F2 plants were mapped using a combination of cleaved amplified polymorphic sequences markers and simple sequence length polymorphisms markers, as described in Lopez-Molina and Chua (2000).

The *ems50-1* locus was mapped to a 1-Mbp interval on chromosome 5 (5.4–6.5 Mbp). After confirmation of the mutation using crosses to T-DNA insertion lines, *ems50-1* was back-crossed using wild-type pollen three times to reduce chances of multiple mutations. All data in this study were acquired using this back-crossed material.

Growth Analyses

Arabidopsis seeds were surface-sterilized, plated, and stratified in darkness at 4°C for 4 d, then seedlings were grown under the specified conditions and root length, hypocotyl length, cotyledon surface area, and rosette surface area were measured using the software ImageJ (https://imagej.nih.gov/ij/). For skotomorphogenic growth, plates were left in the light for 4 h after stratifications, then wrapped in aluminum foil and kept in dark conditions. Flowering time was determined by number of rosette leaves at time of bolting. Yield was determined by total seed weight. All analyses were performed using a minimum of 15 individuals, repeated at least three times.

Seed Analyses

Seed size was measured using the software ImageJ. Both seed weight and size were determined by averaging more than 200 seeds in triplicates.

Fatty Acid Methyl Ester Quantification

Dry seeds of wild-type and *cpna2-4* that developed at 22°C and 10°C were collected and used for the analysis (100 seeds, in triplicates). Arabidopsis seed fatty acids were determined as fatty acid methyl esters (FAMEs) using 100 seeds and 25 μg of 1,2,3-triheptadecanoylglycerol (Sigma-Aldrich) as an internal standard. The transesterification reaction and FAME extraction were performed in 7-mL glass tubes fitted with a Teflon liner. Lipids were transesterified from intact seeds using 1 mL of 5% (v/v) H_2SO_4 in MeOH containing 0.05% (w/v) butylated hydroxytoluene and 0.6 mL of toluene. Samples were incubated for 45 min at 85°C in a dry bath. The reaction was stopped by cooling tubes at room temperature. After a brief centrifugation, FAMEs were extracted with 1 mL of NaCl 0.9% (w/v) and 2 mL of *n*-hexane. Samples were thoroughly mixed for 5 min and the upper *n*-hexane phase was recovered by centrifugation (1,500*g* for 5 min). The *n*-hexane phase was transferred into a second glass tube with a Pasteur pipette and the extraction was repeated two additional times. Combined *n*-hexane phases were evaporated to dryness with a flow of nitrogen and FAMEs were resuspended into 200 μL of heptane. FAMEs were analyzed by the gas chromatography-flame ionization detector-analytical technique as described in Pellaud et al. (2018) using 2 μL injected with a split ratio of 1:50. FAME amounts were determined using FAME calibration curves built with the 37 component FAME mix (Supelco).

Chlorophyll Extraction and Measurement

For chlorophyll extraction from cotyledons or leaves, samples were harvested by weight and put in 1 mL of dimethylformamide. For chlorophyll extraction from seeds, embryos, or integuments, 10 seeds were harvested from each silique and put in 10 μL of dimethylformamide. Samples were kept overnight at 4°C then mixed by vortexing and centrifuged for 1 min at 14,000*g*. The supernatant was used to quantify chlorophyll content in a Nanodrop at 647 nm and 664 nm. Values were reported by Zhang and Huang (2013) as:

$$\text{Total chlorophyll content} = 17.9 \times A_{647} + 8.08 \times A_{664}$$

Chlorophyll Fluorescence

Chlorophyll fluorescence was monitored using LED light source and a charge-coupled device camera (Speedzen System; JBeamBio). Maximum fluorescence, F_m, was measured with a 250-ms saturating flash. The φ_{PSII} measurements were performed on mature-green seeds, mature-green embryos, seedlings, or rosettes, which were dark-adapted for 20 min before starting the measurement. Samples were adapted for 5 min to the increasing light intensities, allowing φ_{PSII} values to stabilize before the measurement.

Values were calculated using the following equations (Maxwell and Johnson, 2000):

$$F_v/F_m = V_m - F_0/F_m$$

$$\Phi\text{PSII} = F_m' - F'/F_m'$$

$$\text{NPQ} = F_m - F_m'/F_m'$$

ECS

In vivo spectroscopic measurements were performed with a JTS10 Spectrophotometer (Bio-Logic). The amount of functional photosynthetic complexes was evaluated measuring the ECS, i.e. a modification of the absorption bands of photosynthetic pigments that is linearly correlated to the number of light-induced charge separations within the photosynthetic complexes (Bailleul et al., 2010). Photosystems content were estimated from the amplitude of the fast (500 μs) phase of the ECS signal (at 520–546 nm) upon excitation with a Xenon flash lamp (duration 15 μs).

Photosynthetic electron flow rates were calculated from the relaxation kinetics of the ECS signal in the dark (Sacksteder et al., 2000; Joliot and Joliot, 2002). Shortly, under steady-state illumination, the ECS signal results from electron transfer through the PSII, cytochrome b6f complex, and PSI complex and from transmembrane potential dissipation via ATP synthesis. After illumination, electron flow is stopped. Therefore, the difference between the slopes of the ECS signal measured in the dark and in the light corresponds to the rate of "total" electron flow. This can be quantified by dividing the difference in the slope (light minus dark) by the amplitude of the ECS signal measured after the Xenon flash illumination (see above).

Immunoblot Analysis

Wild-type or *cpna2-4* seedlings or embryos were homogenized with homogenization buffer (0.0625 M of Tris-HCl at pH 6.8, 1% [w/v] SDS, 10% [v/v] glycerol, and 0.01% [v/v] 2-mercaptoethanol), and total proteins were separated by SDS-PAGE and transferred to a PVDF membrane (Amersham). LHCA1 (Agrisera), LHCB1 (Agrisera), and UGPase (Agrisera) proteins were detected using corresponding antibodies at 1:5,000 dilution. Antibodies against PsaD, D1, and RbcS were a gift of Michel Goldschmidt-Clermont and Jean-David Rochaix. PsaD, D1, and RbcS proteins were detected using corresponding antibodies at 1:2,500 dilution. For all antibodies, anti-rabbit IgG HRP-linked whole antibody (GE Healthcare) in a 1:10,000 dilution was used as a secondary antibody.

Confocal Microscopy

Fluorescence signals were detected with a model no. TCS SP5 STED CW confocal microscope using a ×40 oil immersion objective lens (N.A. = 0.8; Leica). Samples were imaged in water supplemented with propidium iodide (PI, 10 μg/mL). PI and chlorophyll were excited with the 561-nm and 488-nm laser, respectively. The fluorescence emission was collected at 575 nm for PI and between 650-nm and 675-nm band-pass for chlorophyll.

Chloroplast Size/Density Measurement

Confocal images were analyzed using the software ImageJ. A minimum of 800 chloroplasts from six different embryos were measured to determine chloroplast size. A minimum of 150 cells from six different embryos were analyzed to determine average cell area and chloroplast number. Values are reported as:

$$\text{chloroplast density} = (\text{average \# of chloroplasts per cell})/(\text{average cell surface area})$$

Accession Numbers

Sequence data from this article can be found in the GenBank/EMBL (https://www.ncbi.nlm.nih.gov/genbank/) data libraries under accession numbers AT5G18820 (CPN60a2), AT2G28000 (CPN60a1), AT4G02510 (TOC159), AT2G34640 (HMR), AT2G48120 (PAC), AT3G26900 (SKL1), AT4G24770 (CP33a).

Supplemental Data

The following supplemental materials are available.

Supplemental Figure S1. The *ems50-1* mutant phenotype is caused by A to G substitution present in *CPN60α2* (AT5G18820).

Supplemental Figure S2. *cpna2-4* mutant seedlings exhibit a temperature-sensitive phenotype.

Supplemental Figure S3. Photosynthetic efficiency parameters in rosettes of wild-type and *cpna2-4* mutant plants at the 10-leaf rosette stage and 7 d after transfer to cold.

Supplemental Figure S4. PSII quantum efficiency (ΦPSII) as a function of light intensity (μE m-2 s^{-1}) in wild-type and *cpna2-4* seedlings after 40 d of growth at 10°C.

Supplemental Figure S5. PSII quantum efficiency (ΦPSII) as a function of light intensity (μE m-2 s^{-1}) in cotyledons of wild-type and *cpna2-4* seedlings grown at 22°C for 6 d and after an additional 14 d at 10°C.

Supplemental Figure S6. Photosynthetic parameters in developing *cpna2-4* mutant embryos.

Supplemental Figure S7. Developing *cpna2-4* mutant seeds accumulate low chlorophyll levels under low temperatures.

Supplemental Figure S8. Accumulation of core PSI (PsaD and LHCA1), PSII (D1 and LHCB1), and RbcS proteins in embryos of wild-type and *cpna2-4* maturing at 22°C or 10°C.

Supplemental Figure S9. Fatty acid content in wild-type and *cpna2-4* seeds developing at either 22°C or 10°C.

Supplemental Figure S10. Germination percentage of 22°C- wild-type, 10°C- wild-type, 22°C-*cpna2-4*, and 10°C-*cpna2-4* seeds after a stratification period of 4 d.

Supplemental Figure S11. Analysis of 22°C- wild-type, 10°C- wild-type, 22°C-*cpna2-4*, and 10°C-*cpna2-4* plant development over time.

Supplemental Figure S12. Cold-induced developmental defects are unrelated to the maternal genotype.

Supplemental Figure S13. *cpna2-4* developing seeds are unaffected by a short exposure to cold.

Supplemental Figure S14. Cold applied to photosynthetically active *cpna2-4* embryos does not induce developmental defects.

Supplemental Figure S15. *cpna1-2* is a temperature-sensitive mutation that phenocopies *cpna2-4*.

Supplemental Figure S16. Mutants defective in embryonic photosynthesis suffer from skotomorphogenic growth defects.

Supplemental Figure S17. DCMU-treated developing seeds of different Arabidopsis accessions produce seedlings with developmental defects.

ACKNOWLEDGMENTS

We thank Toshiharu Shikanai, Felix Kessler, and Christian Schmitz-Linneweber for sharing plant material. We thank Michel Goldschmidt-Clermont for helpful discussions. We thank Michel Goldschmidt-Clermont and Jean-David Rochaix for providing antibodies. We thank all members of the Luis Lopez-Molina laboratory for discussions.

Received January 16, 2020; accepted January 28, 2020; published February 14, 2020.

LITERATURE CITED

Allorent G, Osorio S, Vu JL, Falconet D, Jouhet J, Kuntz M, Fernie AR, Lerbs-Mache S, Macherel D, Courtois F, et al (2015) Adjustments of embryonic photosynthetic activity modulate seed fitness in *Arabidopsis thaliana*. New Phytol **205:** 707–719

Bailleul B, Cardol P, Breyton C, Finazzi G (2010) Electrochromism: A useful probe to study algal photosynthesis. Photosynth Res **106:** 179–189

Borisjuk L, Rolletschek H (2009) The oxygen status of the developing seed. New Phytol **182:** 17–30

Chan KX, Phua SY, Crisp P, McQuinn R, Pogson BJ (2016) Learning the languages of the chloroplast: Retrograde signaling and beyond. Annu Rev Plant Biol **67:** 25–53

Chen M, Galvão RM, Li M, Burger B, Bugea J, Bolado J, Chory J (2010) Arabidopsis HEMERA/pTAC12 initiates photomorphogenesis by phytochromes. Cell **141:** 1230–1240

Crosatti C, Rizza F, Badeck FW, Mazzucotelli E, Cattivelli L (2013) Harden the chloroplast to protect the plant. Physiol Plant **147:** 55–63

Hobbs DH, Flintham JE, Hills MJ (2004) Genetic control of storage oil synthesis in seeds of Arabidopsis. Plant Physiol **136:** 3341–3349

Holding DR, Springer PS, Coomber SA (2000) The chloroplast and leaf developmental mutant, pale cress, exhibits light-conditional severity and symptoms characteristic of its ABA deficiency. Ann Bot **86:** 953–962

Hua W, Li RJ, Zhan GM, Liu J, Li J, Wang XF, Liu GH, Wang HZ (2012) Maternal control of seed oil content in *Brassica napus*: The role of silique wall photosynthesis. Plant J **69:** 432–444

Iwasaki M, Hyvärinen L, Piskurewicz U, Lopez-Molina L (2019) Non-canonical RNA-directed DNA methylation participates in maternal and environmental control of seed dormancy. eLife **8:** 1–17

Johnson MP (2016) Photosynthesis. Essays Biochem **60:** 255–273

Joliot P, Delosme R (1974) Flash-induced 519 nm absorption change in green algae. Biochim Biophys Acta Bioenerg **357:** 267–284

Joliot P, Joliot A (2002) Cyclic electron transfer in plant leaf. Proc Natl Acad Sci USA **99:** 10209–10214

Ke X, Zou W, Ren Y, Wang Z, Li J, Wu X, Zhao J (2017) Functional divergence of chloroplast Cpn60α subunits during Arabidopsis embryo development. PLoS Genet **13:** e1007036

Kim C, Lee KP, Baruah A, Nater M, Göbel C, Feussner I, Apel K (2009) $^1O_2$-mediated retrograde signaling during late embryogenesis predetermines plastid differentiation in seedlings by recruiting abscisic acid. Proc Natl Acad Sci USA **106:** 9920–9924

Lee KP, Kim C, Landgraf F, Apel K (2007) EXECUTER1- and EXECUTER2-dependent transfer of stress-related signals from the plastid to the nucleus of *Arabidopsis thaliana*. Proc Natl Acad Sci USA **104:** 10270–10275

Leprince O, Pellizzaro A, Berriri S, Buitink J (2017) Late seed maturation: Drying without dying. J Exp Bot **68:** 827–841

Liebers M, Grübler B, Chevalier F, Lerbs-Mache S, Merendino L, Blanvillain R, Pfannschmidt T (2017) Regulatory shifts in plastid transcription play a key role in morphological conversions of plastids during plant development. Front Plant Sci **8:** 23

Liu H, Wang X, Ren K, Li K, Wei M, Wang W, Sheng X (2017) Light deprivation-induced inhibition of chloroplast biogenesis does not arrest embryo morphogenesis but strongly reduces the accumulation of storage reserves during embryo maturation in Arabidopsis. Front Plant Sci **8:** 1287

Liu X, Zhou Y, Xiao J, Bao F (2018) Effects of chilling on the structure, function and development of chloroplasts. Front Plant Sci **9:** 1715

Lopez-Molina L, Chua NH (2000) A null mutation in a bZIP factor confers ABA-insensitivity in *Arabidopsis thaliana*. Plant Cell Physiol **41:** 541–547

Maxwell K, Johnson GN (2000) Chlorophyll fluorescence—a practical guide. J Exp Bot **51:** 659–668

Nater M, Apel K, Kessler F, op den Camp R, Meskauskiene R, Goslings D (2002) FLU: A negative regulator of chlorophyll biosynthesis in *Arabidopsis thaliana*. Proc Natl Acad Sci USA 10.1073/pnas.221252798

op den Camp RG, Przybyla D, Ochsenbein C, Laloi C, Kim C, Danon A, Wagner D, Hideg É, Göbel C, Feussner I, et al (2013) Rapid induction of singlet oxygen in Arabidopsis. Plant Cell **15:** 2320–2332

Pellaud S, Bory A, Chabert V, Romanens J, Chaisse-Leal L, Doan AV, Frey L, Gust A, Fromm KM, Mène-Saffrané L (2018) WRINKLED1 and ACYL-COA:DIACYLGLYCEROL ACYLTRANSFERASE1 regulate tocochromanol metabolism in Arabidopsis. New Phytol **217:** 245–260

Peng L, Fukao Y, Myouga F, Motohashi R, Shinozaki K, Shikanai T (2011) A chaperonin subunit with unique structures is essential for folding of a specific substrate. PLoS Biol **9:** e1001040

Pogson BJ, Ganguly D, Albrecht-Borth V (2015) Insights into chloroplast biogenesis and development. Biochim Biophys Acta Bioenerg **1847:** 1017–1024

Puthur JT, Shackira AM, Saradhi PP, Bartels D (2013) Chloroembryos: A unique photosynthesis system. J Plant Physiol **170:** 1131–1138

Rolletschek H, Weber H, Borisjuk L (2003) Energy status and its control on embryogenesis of legumes. Embryo photosynthesis contributes to oxygen supply and is coupled to biosynthetic fluxes. Plant Physiol **132:** 1196–1206

Sacksteder CA, Kanazawa A, Jacoby ME, Kramer DM (2000) The proton to electron stoichiometry of steady-state photosynthesis in living plants: A proton-pumping Q cycle is continuously engaged. Proc Natl Acad Sci USA **97:** 14283–14288

Scholl RL, May ST, Ware DH (2000) Seed and molecular resources for Arabidopsis. Plant Physiol **124:** 1477–1480

Shanmugabalaji V, Chahtane H, Accossato S, Rahire M, Gouzerh G, Lopez-Molina L, Kessler F (2018) Chloroplast biogenesis controlled by DELLA-TOC159 interaction in early plant development. Curr Biol **28:** 2616–2623.e5

Tada A, Adachi F, Kakizaki T, Inaba T (2014) Production of viable seeds from the seedling lethal mutant ppi2-2 lacking the atToc159 chloroplast protein import receptor using plastic containers, and characterization of the homozygous mutant progeny. Front Plant Sci **5:** 243

Tejos RI, Mercado AV, Meisel LA (2010) Analysis of chlorophyll fluorescence reveals stage specific patterns of chloroplast-containing cells during Arabidopsis embryogenesis. Biol Res **43:** 99–111

ten Hove CA, Lu K-J, Weijers D (2015) Building a plant: Cell fate specification in the early Arabidopsis embryo. Development **142:** 420–430

Teubner M, Fuß J, Kühn K, Krause K, Schmitz-Linneweber C (2017) The RNA recognition motif protein CP33A is a global ligand of chloroplast mRNAs and is essential for plastid biogenesis and plant development. Plant J **89:** 472–485

Vitlin Gruber A, Vugman M, Azem A, Weiss CE (2018) Reconstitution of pure chaperonin hetero-oligomer preparations *in vitro* by temperature modulation. Front Mol Biosci **5:** 5

Wagner D, Przybyla D, op den Camp R, Kim C, Landgraf F, Lee KP, Wursch M, Laloi C, Nater M, Hideg E, et al (2004) The genetic basis of singlet oxygen-induced stress responses of *Arabidopsis thaliana*. Science **306:** 1183–1185

Zhang Z, Huang R (2013) Analysis of malondialdehyde, chlorophyll proline, soluble sugar, and glutathione content in Arabidopsis seedling. Bio Protoc **3:** 2–10